

## Influence of residual surface stress on the fracture of nanoscale piezoelectric materials with conducting cracks

NAN HaiShun & WANG BaoLin\*

*Graduate School at Shenzhen, Harbin Institute of Technology, Harbin 150001, China*

Received January 5, 2013; accepted April 15, 2013; published online December 23, 2013

In this paper, we analyze the stress and electric field intensity factors affected by residual surface stress for conducting cracks in piezoelectric nanomaterials. The problem is reduced to a system of non-linear singular integral equations, whose solution is determined by iteration technique. Numerical results indicate that the residual surface stress can significantly alter the crack tip fields at nanometer length scales. Due to the residual surface stress, the electric field can produce stress around crack tip. This suggests a strong electromechanical coupling crack tip field for nanoscale piezoelectric materials. Such a finding is considerably different from the classical fracture mechanics results. A transit electric field to stress load ratio is identified, for which influences of residual surface stresses vanish. The research is useful for the applications of nanoscale piezoelectric devices.

**fracture mechanics, residual surface stress, piezoelectric materials, nanomechanics, conducting cracks**

**PACS number(s):** 85.85.+j, 68.35.md, 68.03.cd, 46.50.+a

**Citation:** Nan H S, Wang B L. Influence of residual surface stress on the fracture of nanoscale piezoelectric materials with conducting cracks. *Sci China-Phys Mech Astron*, 2014, 57: 280–285, doi: 10.1007/s11433-013-5250-y

### 1 Introduction

The understanding of the fracture mechanisms of devices with nanosized defects such as cavities and cracks has aroused much attention in research works. Some experiments and simulations have been done to focus on the issue. For example Huang et al. [1] explore the mechanical behavior of nanoscale cracks by atomistic analysis, and Belytschko et al. [2] deal with nanotube fracture by applying the atomistic simulations. Several theoretical methods have been developed to demonstrate the problem. Ou et al. [3] investigated the problem of a nanosized spheroidal cavity by considering the residual surface stress. Duan et al. [4] worked out elastostatic solutions to the problem of a nano inhomogeneity.

Along with the nanotechnology development, piezoelectric nanostructured materials now can be successfully fabricated with great potential applications. Many nanodevices are based on piezoelectric nanostructured materials, such as nanosensors, nanoresonators and nanogenerators [5–7]. For promising applications in nanoscale devices, an important research topic is to analyze the deformation and failure behavior of piezoelectric nanomaterials. However, due to the large surface-to-volume ratio, the electromechanical behavior of the piezoelectric nanostructured materials often exhibits distinct size dependence [8,9]. Many researchers have studied the surface effect on the mechanical properties of nanostructures by using the continuum mechanics model of surface elasticity developed by Gurtin and Murdoch [10] and Gurtin et al. [11]. For example, the natural frequency of nanobeam affected by surface elasticity has been investigated by Gurtin et al. [12]. Buckling and vibration study of piezoelectric nanowires with the consideration of residual

\*Corresponding author (email: wangbl@hitsz.edu.cn)

surface stress was performed by Wang et al. [13]. Thus, how residual surface stresses affect the cracking of nanoscale piezoelectric material is a valuable task for design and manufacture of piezoelectric devices at nanoscale.

Although many researches have been done in the field of fracture problems for piezoelectric macrostructure [14,15], studies about the surface effect on fracture behaviors of piezoelectric nanomaterials with conducting cracks is still very limited. As a parameter to measure fracture behaviors of the materials, the crack tip field intensity factor is essential for evaluating the reliability and estimating the residual life of the structures. Thus this paper analyzes the influence of residual surface stress on the energy release rate, stress and electric field intensity factors for a conducting crack in an infinite piezoelectric nanomaterial. We proposed the expressions of energy release rate and field intensity factors with the consideration of residual surface stresses on the whole crack surface. A continuum modeling of elastic nanostructures is used. The problem is nonlinear and is solved by the numerical iteration method. The result indicates residual surface stresses reduce the energy release rate and crack tip field intensity factors if residual surface stresses are positive. However, the electric field intensity factor is found to have no correlation with the residual surface effect, which is also consistent with the classic fracture mechanics theory.

## 2 Formulation of the problem

Considered is a problem of an infinite piezoelectric nanomaterials containing a crack lying along the poling axis ( $x$  axis) shown in Figure 1(a), where  $(x, y)$  is a coordinate system. The length of crack is  $2a$ . It is a symmetric problem about the  $y=0$  plane. We study the plane problem so that all field variables are assumed to be functions of  $x$  and  $y$  only. The medium is subjected to a uniform electric field  $E_\infty$  in the  $x$  direction and a normal stress  $\sigma_\infty$  perpendicular to the

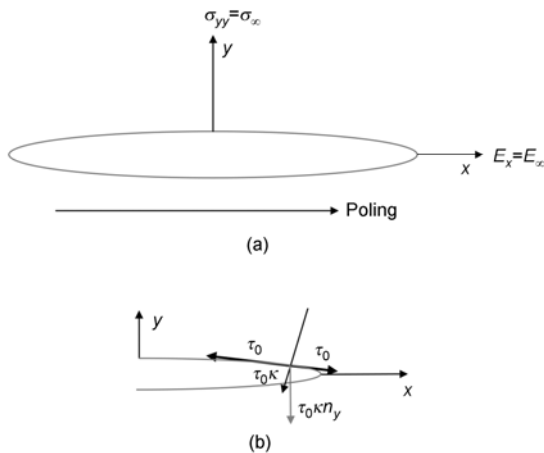


**Figure 1** (a) A crack of length  $2a$  in an infinite piezoelectric nanomaterials. (b) The residual surface stress on the crack surface.

direction of  $E_\infty$  at infinity. The crack is free of mechanical forces and electrically conducting. Mathematically, the boundary conditions of the crack surface can be read as:

$$\sigma_{yy}(x, 0) = 0, E_x(x, 0) = 0, |x| < a. \quad (1)$$

According to Cammarata [16] and Gibbs [17], the surface tensor  $\sigma_{\alpha\beta}^s$  can be defined as  $\sigma_{\alpha\beta}^s = \gamma\delta_{\alpha\beta} + \partial\gamma / \partial\varepsilon_{\alpha\beta}^s$ , where  $\gamma$  is the surface energy density,  $\varepsilon_{\alpha\beta}^s$  is the surface strain tensor and  $\delta_{\alpha\beta}$  is the Kronecker. In this problem, the one-dimensional form is used to describe the crack surface stress, that is,  $\sigma^s = E^s\varepsilon + \tau_0$ , where  $E^s$  is the surface Young's modulus and  $\tau_0$  is the residual surface stress under unstrained case. The contribution of the component of  $E^s\varepsilon$  can be neglected compared with that of  $\tau_0$  [3,18] when the deformed atomic spacing changing infinitesimally. Then the surface stresses on the crack surface are governed by  $\tau_0$  as shown in Figure 1(b), where the direction of  $\tau_0$  is tangent to the crack surface. According to the equilibrium conditions on the surface, the residual surface stress induces a transverse loading at any point  $o$  on the crack surface, which can be expressed as  $\tau_0\kappa$ , where  $n_o$  is the unit normal vector at point  $o$  and  $\kappa$  is the surface curvature tensor. The fact that  $\tau_0$  can produce a load perpendicular to the crack face is demonstrated in Figure 1(b). Obviously, the load generated by  $\tau_0$  along the  $y$  axis is  $\tau_0\kappa n_y$ , where  $n_y$  is the orientation cosine of the vector normal to the crack surface.

## 3 Solution to the problem

Numerous references are related to solve the crack problem in piezoelectric medium [19]. Using Fourier integrals and characteristic equation, the stress and the electric field function can be derived. By introducing the auxiliary functions that satisfy the boundary conditions, the crack tip fields can be obtained by solving a system of singular integral equations. Analog to solutions for piezoelectric crack problem [20], we introduce auxiliary functions  $g_\phi(x)$  and  $g_V(x)$  along the crack plane, where  $g_\phi(x) = 2\partial\phi(x, 0) / \partial x$ ,  $g_V(x) = 2\partial V(x, 0) / \partial x$ ,  $\phi$  is electric potential and  $V$  is the crack face displacement in the  $y$ -direction. From the geometry analysis, the orientation cosine for the vector normal to the crack surface  $n_y$  and the radius of crack surface curvature  $\rho$  can be expressed by  $g_V$  as:

$$n_y = 1 / \sqrt{1 + g_V'^2 / 4} \quad (2)$$

and

$$\rho = 1 / \kappa = -2(1 + g_V'^2 / 4)^{3/2} / g_V''. \quad (3)$$

According to Gurtin et al. [10–12], the presence of residual surface stress only results in non-classical boundary

conditions. It does not change any other governing equations. Thus by incorporating the residual surface stress  $\tau_0$  and with the aid of singular integral equation method [21], the electric field and stress in terms of  $g_\phi(r)$  and  $g_V(r)$  on the  $y=0$  plane can be expressed as:

$$\begin{aligned} \begin{Bmatrix} \sigma_{yy}(x,0) \\ E_x(x,0) \end{Bmatrix} &= \frac{[\Lambda]}{\pi} \int_{-a}^a \frac{1}{(r-x)} \begin{Bmatrix} g_V(r) \\ g_\phi(r) \end{Bmatrix} dr \\ &+ \begin{Bmatrix} \sigma_\infty - \frac{\tau_0 n_y(x)}{\rho(x)} \\ E_\infty \end{Bmatrix}, \end{aligned} \tag{4}$$

where  $[\Lambda] = \begin{bmatrix} \Lambda_{11} & \Lambda_{12} \\ \Lambda_{21} & \Lambda_{22} \end{bmatrix}$  only related to material's properties is a (2x2) symmetric matrix [19]. Eq. (4) gives the stress and electric displacement inside and outside the crack. For inside the crack,  $|x| < a$ , eq. (4), together with the boundary conditions (1), gives

$$\frac{[\Lambda]}{\pi} \int_{-a}^a \frac{1}{(r-x)} \begin{Bmatrix} g_V(r) \\ g_\phi(r) \end{Bmatrix} dr + \begin{Bmatrix} \sigma_\infty - \frac{\tau_0 n_y(x)}{\rho(x)} \\ E_\infty \end{Bmatrix} = \begin{Bmatrix} 0 \\ 0 \end{Bmatrix}, \tag{5}$$

$$|x| \leq a.$$

Eq. (5) are Cauchy-type singular integral equations. Using the method of integral equation [22] and let  $\bar{x} = x/a$  and  $\bar{r} = r/a$ , the solutions to  $g_V(r)$  and  $g_\phi(r)$  related to the Chebyshev polynomials of the first kind  $T_m(\bar{r})$  and unknown constants  $\{C_{Vm}, C_{\phi m}\}^T$  can be expressed as:

$$\begin{Bmatrix} g_V(a\bar{r}) \\ g_\phi(a\bar{r}) \end{Bmatrix} = \sum_{m=1}^{\infty} \begin{Bmatrix} C_{Vm} \\ C_{\phi m} \end{Bmatrix} \frac{T_m(\bar{r})}{\sqrt{1-\bar{r}^2}}, \quad -1 \leq \bar{r} \leq 1, \tag{6}$$

where  $T_m(r/a) = \cos(m \arccos(r/a))$  and  $\{C_{Vm}, C_{\phi m}\}^T$  need to be determined. Eq. (5) are solved by truncating and substituting the first  $M$  terms of eq. (6) into it and using the well-known integral

$$\frac{1}{\pi} \int_{-1}^1 \frac{T_m(\bar{r})}{(\bar{r}-\bar{x})\sqrt{1-\bar{r}^2}} d\bar{r} = U_{m-1}(\bar{x}) \tag{7}$$

for  $m \geq 1$  and  $|\bar{x}| < 1$ , where  $U_{m-1}(\bar{x}) = \sin(m \arccos \bar{x}) / \sqrt{1-\bar{x}^2}$  is the Chebyshev polynomial of the second kind, we can obtain

$$\sum_{m=1}^M \begin{Bmatrix} U_{m-1}(\bar{x}) C_{Vm} \\ U_{m-1}(\bar{x}) C_{\phi m} \end{Bmatrix} = [\bar{\Lambda}] \begin{Bmatrix} -\sigma_\infty + \frac{\tau_0 n_y(\bar{x})}{\rho(\bar{x})} \\ -E_\infty \end{Bmatrix}, \tag{8}$$

where  $[\bar{\Lambda}] = [\Lambda]^{-1} = \begin{bmatrix} \bar{\Lambda}_{11} & \bar{\Lambda}_{12} \\ \bar{\Lambda}_{21} & \bar{\Lambda}_{22} \end{bmatrix}$  is the inverse matrix of

$[\Lambda]$ . To solve eq. (8), for  $-1 \leq x_k \leq 1$  we let  $x_k = \cos[(2k-1)\pi/(2M)]$ ,  $k \in [1, M]$ . The substitutions of  $x_k$  into eq. (8) yield [21]

$$\begin{Bmatrix} S, 0 \\ 0, S \end{Bmatrix} \begin{Bmatrix} C_V \\ C_\phi \end{Bmatrix} = [\bar{\Lambda}] \begin{Bmatrix} T \\ -E_\infty \end{Bmatrix}, \tag{9}$$

where  $\{C_V\}, \{C_\phi\}$  are, respectively, a column whose elements are  $C_{Vm}$  and  $C_{\phi m}$ ;  $\{T\}$  is a column whose elements are  $\left\{-\sigma_\infty + \frac{\tau_0 n_y(x_k)}{\rho(x_k)}\right\}$ ;  $[S]$  is a  $M \times M$  matrix whose elements are

$$(S)_{mn} = U_{n-1}(x_m) = \sin(n \arccos x_m) / \sqrt{1-x_m^2}. \tag{10}$$

After solving eq. (9), we can obtain the solution to  $C_{Vm}$  and  $C_{\phi m}$ . Then the stress and electric field can be derived by  $\{g_V(r), g_\phi(r)\}^T$  in terms of  $\{C_{Vm}, C_{\phi m}\}^T$ . Based on the definitions of the field intensity factors, we have

$$\begin{Bmatrix} K_I \\ K_E \end{Bmatrix} = -[\Lambda] \sqrt{\pi a} \begin{Bmatrix} \sum_{m=1}^M C_{Vm} \\ \sum_{m=1}^M C_{\phi m} \end{Bmatrix}. \tag{11}$$

In fracture mechanics application, energy release rate is a vital aspect to evaluate crack growth behavior. With the expressions of the field intensity factors, we can obtain the energy release rate as [19]:

$$G = \frac{1}{4} \{K_I, K_E\} [\bar{\Lambda}] \begin{Bmatrix} K_I \\ K_E \end{Bmatrix}. \tag{12}$$

Since the influence of residual surface stress has been included in field intensity factors at crack tip,  $G$  will automatically reflect the effect of residual surface stress.

From above analyzes we can find that it is impossible to get the close-form solution to eq. (9) on account of the inclusion of the residual surface stress. However, the closed form solutions can be obtained by taking  $M=1$ . In such a case, we obtain

$$\begin{Bmatrix} g_V(a\bar{r}) \\ g_\phi(a\bar{r}) \end{Bmatrix} = \frac{\bar{r}}{\sqrt{1-\bar{r}^2}} \begin{Bmatrix} C_{V1} \\ C_{\phi 1} \end{Bmatrix}, \tag{13}$$

$$\begin{Bmatrix} V(a\bar{x}, 0) \\ \phi(a\bar{x}, 0) \end{Bmatrix} = -\frac{a\sqrt{1-\bar{x}^2}}{2} \begin{Bmatrix} C_{V1} \\ C_{\phi 1} \end{Bmatrix}.$$

Thus,  $\rho = -2a[1-\bar{r}^2 + C_{V1}^2 \bar{r}^2 / 4]^{3/2} / C_{V1}$  and  $n_y = 1 / \sqrt{1 + C_{V1}^2 \bar{r}^2 / (4 - 4\bar{r}^2)}$ . Finally,  $[S] = 1$ ,  $\rho(0) = -2a / C_{V1}$

and  $n_y=1$ . Substituting the results into eq. (9) gives

$$C_{V1} = -\frac{\bar{\Lambda}_{11}\sigma_\infty + \bar{\Lambda}_{12}E_\infty}{1 + \bar{\Lambda}_{11}\tau_0 / (2a)}, \tag{14a}$$

$$C_{\phi 1} = -\left(\bar{\Lambda}_{21} - \frac{\bar{\Lambda}_{21}\bar{\Lambda}_{11}}{\bar{\Lambda}_{11} + 2a / \tau_0}\right)\sigma_\infty - \left(\bar{\Lambda}_{22} - \frac{\bar{\Lambda}_{21}\bar{\Lambda}_{12}}{\bar{\Lambda}_{11} + 2a / \tau_0}\right)E_\infty. \tag{14b}$$

Accordingly, we can obtain the close-form solutions to field intensity factors

$$K_I = \frac{\sigma_\infty\sqrt{\pi a}}{1 + \bar{\Lambda}_{11}\tau_0 / (2a)} - \frac{\bar{\Lambda}_{12}E_\infty\sqrt{\pi a}}{\bar{\Lambda}_{11} + 2a / \tau_0}, \tag{15a}$$

$$K_E = E_\infty\sqrt{\pi a}. \tag{15b}$$

Based on the above analyses, we can have the normalized results. If the residual surface stress is absent (i.e., in eq. (9) the term  $\tau_0 n_y(\bar{x}) / \rho(\bar{x})$  is neglected), the solutions to  $K_{I_0}$  and  $K_{E_0}$  are given by  $K_{I_0} = \sigma_\infty\sqrt{\pi a}$  and  $K_{E_0} = E_\infty\sqrt{\pi a}$ , which are the field intensity factors without considering the residual surface stress. The corresponding energy release rate can be expressed by  $G_o = \{K_{I_0}, K_{E_0}\} [\bar{\Lambda}] \{K_{I_0}, K_{E_0}\}^T / 4$ . These are well-known classical fracture mechanics solutions. For any piezoelectric material  $E_\infty / \sigma_\infty$  can be expressed by  $\bar{\Lambda}_{11}$ , and then we have

$$\frac{K_I}{K_{I_0}} = \frac{1}{1 + l_c / (2a)} - \frac{\bar{\Lambda}_{12}E_\infty / (\sigma_\infty\bar{\Lambda}_{11})}{1 + 2a / l_c}, \tag{16}$$

which will approach 1 when  $a \gg l_c$ , where  $l_c = \bar{\Lambda}_{11}\tau_0$  is the characteristic length parameter of materials. Under the conditions, we can also have the result  $K_E=K_{E_0}$ . Thus,  $K_E$  does not depend on the residual surface stress on the crack faces.

However, a reasonable accuracy is desired to reach for  $M>1$  in practical applications. Here we exploit an iterative method to calculate the solutions. First, because there are no initial electro-mechanical loads the crack is flat and closed. Then the crack opening is not influenced by residual surface stress. Second, when the crack is opened due to the mechanical and electrical load, a load  $\tau_0 n_y$  would generated by surface stress, which can be determined by crack surface displacement. After solving eq. (9), we can obtain the solutions to  $C_V$  and a new crack surface displacement related to the residual surface. Next repeat the second procedure till solutions converge. In doing so, the solutions to  $C_V$  and  $C_\phi$  in eq. (9) for  $M>1$  will be worked out. The exact solutions will be approximated as  $M$  increases.

### 4 Results and discussion

For numerical illustrations, we chose PZT-4 piezoelectric media to analyze the residual surface effect on the field intensity factor. Their bulk material properties are given by [23]:  $c_{11}=13.9$  ( $10^{10}$  N/m),  $c_{13}=7.43$  ( $10^{10}$  N/m),  $c_{33}=11.3$  ( $10^{10}$  N/m),  $e_{31}=-6.980$  (C/m<sup>2</sup>),  $e_{33}=13.84$  (C/m<sup>2</sup>),  $e_{15}=13.44$  (C/m<sup>2</sup>),  $\epsilon_{11}=60.0$  ( $10^{10}$  C/Vm),  $\epsilon_{33}=54.7$  ( $10^{10}$  C/Vm). After solving the problem as in sect. 3, we can obtain the matrices

$$[\Lambda] = \begin{bmatrix} 2.838 & 0.05338 \\ 0.05338 & 0.005375 \end{bmatrix} \times 10^{10} \quad \text{and} \quad [\bar{\Lambda}] = [\Lambda]^{-1} =$$

$$\begin{bmatrix} 0.4332 & -4.3021 \\ -4.3021 & 228.7543 \end{bmatrix} \times 10^{-10}. \text{ In this work, the residual}$$

surface stress  $\tau_0=110$  N/m is taken for the simulation [24]. Then use the above date, and the characteristic material parameter can be calculated as  $l_c = \bar{\Lambda}_{11}\tau_0 = 4.7652$  nm.

By the iteration algorithm as mentioned in sect. 3, we know that  $K_E$  is not depending on the residual surface stress. Therefore, only the stress intensity factor influenced by residual surface stresses needs to be discussed. To clearly understand such an effect, we focus our discussions on three cases: pure stress load  $\sigma_\infty$ , pure electric field  $E_\infty$  and combined application of electric field and stress.

For the case of pure stress load, the normalized stress intensity factor  $K_I/K_{I_0}$  as a function of  $all_c$  is plotted in Figure 2. Here  $K_{I_0}$  is  $K_{I_0} = \sigma_\infty\sqrt{\pi a}$  according to sect. 3. Clearly we find that in this case  $K_I/K_{I_0}$  is only related to  $all_c$  rather than the remote applied stress load and that all the values of  $K_I/K_{I_0}$  approach 1 as the half length of crack  $a$  increases. That is, the influence of the residual surface stress on the stress intensity factor becomes weak or even vanishes as a certain crack length is reached. Thus, the effect of residual surface stresses is dramatic and should be taken into consideration when the crack length is reduced to nanoscale.

When the piezoelectric medium is subjected to a pure electric field  $E_\infty$ , Figure 3 displays the stress intensity factor influenced by residual surface stresses, where  $K_I$  has been normalized by  $K_c = \bar{\Lambda}_{12}E_\infty\sqrt{\pi a} / \bar{\Lambda}_{11}$ . The curve for  $M \gg 7$  is supposed to be good agreement with the exact solution. From Figure 3, it is found that the stress intensity factor will run to zero when the crack length increases. These results imply that in consideration of residual surface stress, the application of an electrical field load will generate the stress intensity factor. This is different from the knowledge from the classical fracture mechanics results of linear piezoelectric elasticity that the in the crack plane electric field alone cannot produce the mechanical stress [14,15,19].

The variation of  $K_I/K_{I_0}$  with  $all_c$  for combined electric field  $E_\infty$  and stress load  $\sigma_\infty$  is shown in Figure 4, where  $K_{I_0}$  is prescribed as  $K_{I_0} = \sqrt{\pi a}\sigma_\infty$ . According to eq. (16), we let  $B_\infty = \bar{\Lambda}_{12}E_\infty / (\sigma_\infty\bar{\Lambda}_{11})$ . Then applying the iteration

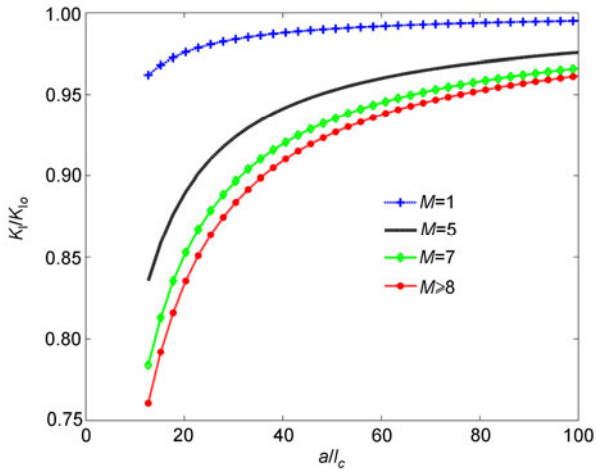


**Figure 2** (Color online) Normalized crack tip stress intensity factor versus normalized half crack length ( $E_\infty=0$ ).

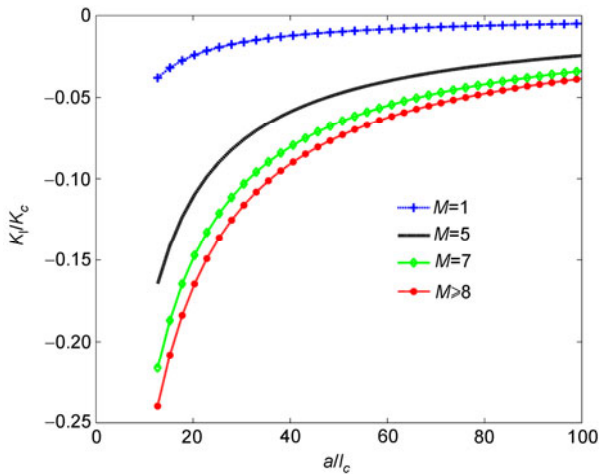


**Figure 3** (Color online) Normalized crack tip stress intensity factor versus of normalized half crack length ( $\sigma_\infty=0$ ).

technique, for different values of  $B_\infty$ , Figure 4 gives the relation of the normalized crack length and normalized stress intensity factor. According to the former researchers who have given the reasonable range of  $B_\infty$  ratio [25], we set  $B_\infty=-2, 0$  and  $2$ . From Figure 4,  $K_I/K_{I0}$  increases with increasing  $all_c$  when  $B_\infty=0$  and  $2$  while it decreases with increasing  $all_c$  for  $B_\infty=-2$ . The result, combining eq. (16), shows that a transit electric field to stress load ratio exists for which the function of residual surface stresses on  $K_I$  vanishes:

$$B_\infty = -1. \tag{17}$$

Specifically, for  $B_\infty < -1$ , the value of stress intensity factor increases due to the residual surface stress. However, for  $B_\infty > -1$  the residual surface stresses decrease the value of  $K_I$ . The information is useful for the determination of an appropriate electric field to mechanical load ratio for piezoelectric devices.

Finally, the energy release rate influenced by residual surface stress is discussed for three cases as shown in Figures 5–7. Correspondingly  $G_o$  for these three figures are calculated as  $G_o = K_{I0}^2 \bar{\Lambda}_{11}$ ,  $G_o = K_{Eo}^2 \bar{\Lambda}_{22}$  and  $G_o = K_{I0}^2 \bar{\Lambda}_{11}$ , respectively. It can be seen that curves for  $M > 8$  are convergent and can be considered as the exact solutions of energy release rate. It can be seen that for all the cases, the existence of the residual surface stress will decrease the energy release rate. Figure 7 shows that by considering residual surface stresses, the electric field will always increase the crack tip energy release rate whatever direction of the electric field. Influences of residual surface stresses on the energy release rate become more prominent with a decrease of crack length.

### 5 Conclusion

Understanding how the residual surface stress influences the

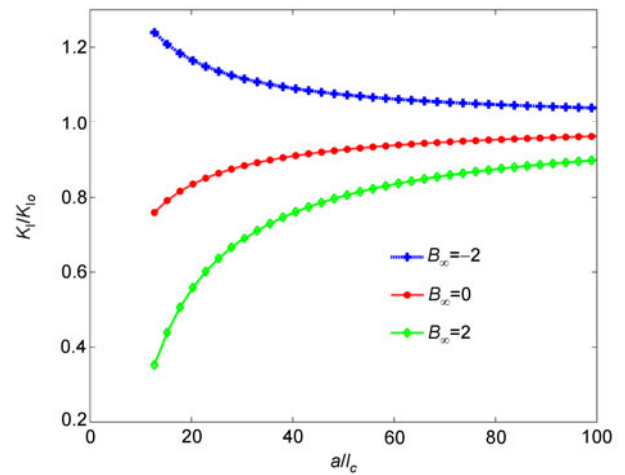


**Figure 4** (Color online) Normalized crack tip stress intensity factor versus of normalized half crack length ( $B_\infty=-2,0,2$ ).

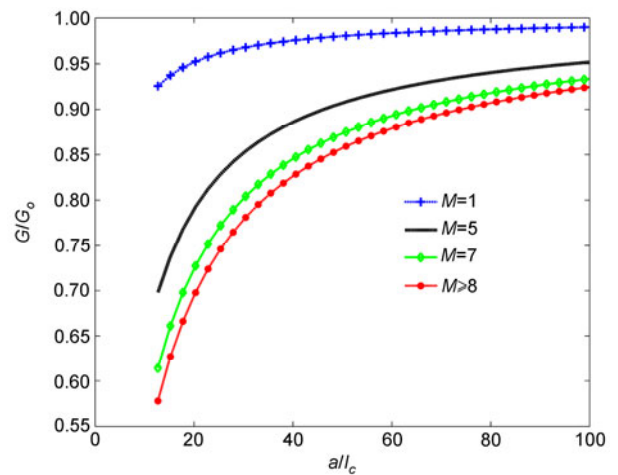


**Figure 5** (Color online) Normalized crack tip energy release rate versus of normalized half crack length ( $E_\infty=0$ ).

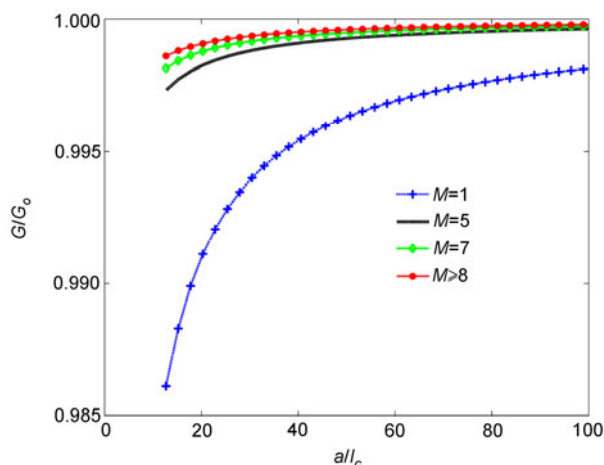


**Figure 6** (Color online) Normalized crack tip energy release rate versus of normalized half crack length ( $\sigma_\infty=0$ ).

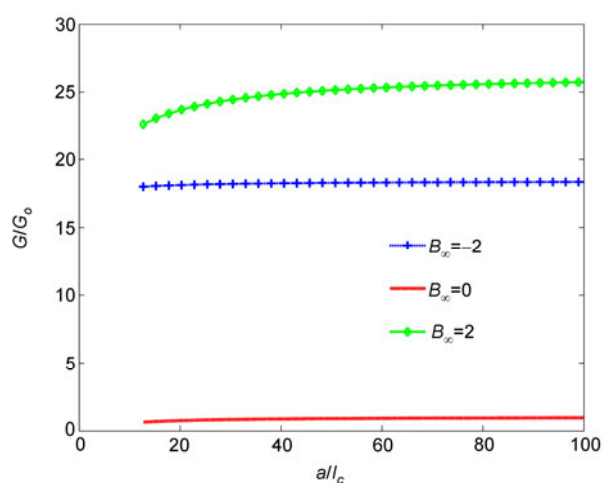


**Figure 7** (Color online) Normalized crack tip energy release rate versus normalized half crack length ( $B_\infty=-2,0,2$ ).

fracture behavior of piezoelectric nanomaterials is essential for tailoring their mechanical properties. This paper studies the residual surface stress on the fracture mechanics parameters of piezoelectric nanomaterials with a conducting crack. The residual surface stress is included in the governing equations by the surface continuum theory. The solutions to the stress intensity factor and the electric field intensity factor are determined through the iteration method. The solutions show that there is no effect on the electric field intensity factor  $K_E$  when the residual surface stress exists. However, the stress intensity factor is greatly affected by the residual surface stress. Moreover, by including residual surface stresses, the electric field can cause crack tip stress intensity factor, which is different from results of the linear piezoelectric crack problem. There exists a transit electric field to stress load ratio for which the influence of residual surface stresses vanish. Influences of residual surface stress on energy release rate are also studied and it is found to be remarkable at nanoscale. These results are envisaged to be helpful for the design piezoelectric nano-devices in NEMS.

This work was supported by the National Natural Science Foundation of China (Grant Nos. 11172081 and 11372086) and Shenzhen Research Innovation Fund, China (Grant No. JCYJ20120613150312764).

- Huang S, Zhang S L, Belytschko T, et al. Mechanics of nanocrack: fracture, dislocation emission, and amorphization. *J Mech Phys Solids*, 2009, 57: 840–850
- Belytschko T, Xiao S P, Schatz G C, et al. Atomistic simulations of nanotube fracture. *Phys Rev B*, 2002, 65(23): 235430
- Ou Z Y, Wang G F, Wang T J. Effect of residual surface tension on the stress concentration around a nanosized spheroidal cavity. *Int J Eng Sci*, 2008, 46: 475–485
- Duan H L, Wang J, Huang Z P, et al. Stress fields of a spheroidal inhomogeneity with an interphase in an infinite medium under remote loadings. *Proc R Soc A*, 2005, 461: 1055–1080
- Caillier C, Ayari A, Gouttenoire V, et al. Gold contact to individual metallic carbon nanotubes: A sensitive nanosensor for high-pressure. *Appl Phys Lett*, 2010, 97: 173111
- Khaderbad M A, Choi Y, Hiralal P, et al. Electrical actuation and readout in a nanoelectromechanical resonator based on a laterally suspended zinc oxide nanowire. *Nanotechnology*, 2012, 23: 025501
- Yang R, Qin Y, Li C, et al. Characteristics of output voltage and current of integrated nanogenerators. *J Mech Phys Solids*, 2009, 94: 022905
- Cuenot S, Fretigny C, Demoustier-Champagne S, et al. Surface tension effect on the mechanical properties of nanomaterials measured by atomic force microscopy. *Phys Rev B*, 2004, 69: 165410
- Jing G Y, Duan H L, Sun X M, et al. Surface effects on elastic properties of silver nanowires: Contact atomic-force microscopy. *Phys Rev B*, 2006, 73(23): 235409
- Gurtin M E, Murdoch A I. A continuum theory of elastic material surfaces. *Arch Ration Mech Anal*, 1975, 57(4): 291–323
- Gurtin M E, Weissmuller J, Larche F. A general theory of curved deformable interfaces in solids at equilibrium. *Philos Mag A*, 1998, 78(5): 1093–1109
- Gurtin M E, Markenscoff X, Thurston R N. Effect of surface stress on the natural frequency of thin crystals. *Appl Phys Lett*, 1976, 29: 529–530
- Wang G F, Feng X Q. Effect of surface stresses on the vibration and buckling of piezoelectric nanowires. *Europhys Lett*, 2010, 91: 56007
- Zhang T Y, Gao C F. Fracture behaviors of piezoelectric materials. *Theor Appl Frac Mec*, 2004, 41: 339–379
- Suo Z, Kuo C M, Barnett D M, et al. Fracture mechanics for piezoelectric ceramics. *Eur J Mech Phys Solids*, 1992, 40: 739–765
- Cammarata R C. Surface and interface stress effects in thin films. *Prog Surf Sci*, 1994, 46(1): 1–38
- Gibbs J W. *The Scientific Papers of J. Willard Gibbs*. Vol. 1: Thermodynamics. New York: Longmans and Green, 1906. 1–413
- Wang G F, Wang T J. Deformation around a nanosized elliptical hole with surface effect. *Appl Phys Lett*, 2006, 89: 161901
- Wang B L, Zhang X H. An electrical field based non-linear model in the fracture of piezoelectric ceramics. *Int J Solids Struct*, 2004, 41: 4337–4347
- Knoda N, Erdogan F. The mixed mode crack problem in a nonhomogeneous elastic plane. *Eng Fract Mech*, 1994, 47: 533–545
- Erdogan F, Gupta G D. On the numerical solution of singular integral equations. *Q Appl Math*, 1972, 29: 525–534
- Muskhelishvili I N. *Single Integral Equations*. Groningen: Noordhoff, 1953. 1–447
- Fulton C C, Gao H J. Electrical nonlinearity in fracture of piezoelectric ceramics. *Appl Mech Rev*, 1997, 50: S56–S63
- Gurtin M E, Murdoch A I. Surface stress in solids. *Int J Solids Struct*, 1978, 14: 431–440
- Wang B L, Noda N. Mixed mode crack initiation in piezoelectric ceramic strip. *Theor Appl Fract Mech*, 2000, 34: 35–47